

Relativistic Model for Radiating Spherical Collapse

Victor Medina¹ and Nelson Falcon²

¹Departamento de Física - Facultad de Ingeniería — Universidad de Carabobo. Valencia, Venezuela
E-mail: vmedina@uc.edu.ve

²Departamento de Física — Facultad Experimental de Ciencias y Tecnología - Universidad de Carabobo. Valencia, Venezuela
E-mail: nelsonfalconv@gmail.com

The relativistic models for radiating spherical collapse is important for to explain the emission process on very high energy in Supernova burst and Quasars. A general method is reviewed, to obtain models which describe non static radiating spheres, without having to make any hypothesis about the emission of radiation during the collapse. It is concluded that the field equations together with the conservation laws (Bianchi's Identity) form a complete set of integrable equations that do not require additional the emissivation hypothesis of a Gaussian pulse on at an arbitrary instant to trigger the collapse. The emissivation hypothesis of a Gaussian pulse is not only unnecessary, but also leads to qualitatively and quantitatively different solutions. Calculations were performed using the computer algebra package *GRTensorII*, running on *Maple 13*, along with several Maple routines that we have used specifically for this type of problems. The Schwarzschild and Tolman VI models are shown as examples where it's emphasizes the importance of using conservation equations properly, for describe the collapse for the self-gravitating sphere.

1 Introduction

The last phases of stellar evolution of massive stars are dominated by the contribution of stellar radiation due to changes of the inner or outer distribution of matter, in the gravitational potential of the radiating fluid spheres and, therefore, general relativity provides a description of the collapse of the compact objects (Neutron Stars, Black Holes). This description can be extended to explain the radiation process of very high energy in astrophysical scenarios, such as Supernova bursts and Quasars. A number of studies have been reported describing a gravitational collapse: Oppenheimer and Snyder [1], Tolman [2] and furthermore the study of the collapsing radiating fluid [3–6].

This scheme has recently been used for various scenarios of relativistic hydrodynamics. We can highlight some examples: charged fluids [7–9], isotropic [10] or anisotropic fluid [11, 12], shock waves [13, 14], in free space [15, 16] or diffusion process [17, 18]. It is necessary to contrast its quantitative results with other calculation schemes. Barreto et al. [19] have extended the semi-numerical scheme to the Schwarzschild coordinates, simulating some scenarios of the gravitational collapse.

Herrera and collaborators [6, 19–21] developed a general algorithm for modeling self gravitating spheres out of equilibrium, beginning from the known static solutions of Einstein's equations. This method divides the space-time in two spatial regions. The outer region is described by the Vaidya solution and the space-time metric in the interior is obtained by solving the Einstein field equations. Further, proper boundary conditions are imposed in order to guarantee a smooth matching of the solutions in the surface of the junction. This semi numerical technique has been used extensively to study high

energy in astrophysical scenarios [19, 21–27].

However in these numerical simulations a Gaussian pulse is introduced *ad hoc* to represent the emission of radiation that initiates the disequilibrium during the collapse of the radiating fluid ball [6, 20, 21, 23–25, 28]. These assumptions could be unnecessary and generate spurious solutions, since this loss of mass is prescribed by one of the conservation equations when applying the Bianchi Identity [29, 30]. Parts of the calculation of the Bianchi identities that were performed in this work were possible and verified using the *GRTensorII* package.

The purpose of this paper is to show the general method to obtain models which describe radiating non-static spheres without having to make any hypothesis about the emission of radiation during the collapse. This paper follows as much as possible the notation and physical description prescribed by Herrera et al. [6]. For this, the field equations and conservation laws are shown in Section 2; then section 3 establishes the procedure for the static solutions and obtaining the surface equations. The models Schwarzschild-like and Tolman VI-like are discussed in section 4 and 5 respectively, and in the last section are shown the concluding remarks.

2 The Field equations and conservation relationships

Let us consider a non static radiating spheres. The metric takes the form [4]

$$ds^2 = e^{2\beta} \frac{V}{r} du^2 + 2e^{2\beta} du dr - r^2 d\theta^2 - r^2 \sin^2 \theta d\phi^2, \quad (1)$$

where u and r are time like and radial-like coordinates respectively; β and V are functions of u and r ; θ, ϕ are the usual angle coordinates. In these coordinates the gravitational field equations are:

$$\begin{aligned}
 -8\pi T_{00} &= -\frac{V_{,0} - 2V\beta_{,0}}{r^2} - \frac{V}{r^3} (e^{2\beta} - V_{,1} + 2\beta_{,1}V) \\
 -8\pi T_{01} &= -\frac{1}{r^2} (e^{2\beta} - V_{,1} + 2\beta_{,1}V) \\
 -8\pi T_{11} &= -\frac{4\beta_{,1}}{r} \\
 -8\pi T_2^2 = -8\pi T_3^3 &= -e^{2\beta} \left(2\beta_{01} - \frac{1}{2r^2} [rV_{,11} + \right. \\
 &\quad \left. - 2\beta_{,1}V + 2r(\beta_{,11}V + \beta_{,1}V_{,1}) \right].
 \end{aligned}$$

As usual, note that we used the subscript $_{,0}$ and $_{,1}$ for the derivative for u and r , respectively; and the semicolon (;) for covariant differentiation. Then transformation relations between local Minkowskian and radiative coordinates are:

$$\begin{aligned}
 dt &= \left(\frac{\partial t}{\partial u}\right) du + \left(\frac{\partial t}{\partial r}\right) dr \\
 &= e^\beta \left(\frac{V}{r}\right)^{\frac{1}{2}} du + e^\beta \left(\frac{r}{V}\right)^{\frac{1}{2}} dr \quad (2)
 \end{aligned}$$

$$dx = \left(\frac{\partial x}{\partial r}\right) dr = e^\beta \left(\frac{r}{V}\right)^{\frac{1}{2}} dr \quad (3)$$

$$dy = \left(\frac{\partial y}{\partial \theta}\right) d\theta = r d\theta \quad (4)$$

$$dz = \left(\frac{\partial z}{\partial \phi}\right) d\phi = r \cdot \sin \theta d\phi. \quad (5)$$

We assumed the stellar material as perfect fluid, with energy density $\hat{\rho}$, radial pressure \hat{P} , without heat conduction neither viscosity, then

$$\hat{T}_{\alpha\beta} = (\hat{\rho} + \hat{P}) \cdot U_\alpha U_\beta - \hat{P} \cdot \eta_{\alpha\beta}, \quad (6)$$

where $U_\alpha = (1, 0, 0, 0)$, $3\hat{\sigma}$ is the isotropic radiation of the energy density, and $\hat{\varepsilon}$ no-polarized component of the energy density in radial direction. Now consider an observer in local Minkowskian system with radial velocity ω , in the Lorentzian system we can write:

$$\bar{T}_{\mu\nu} = \Lambda^\alpha_\mu \Lambda^\beta_\nu \hat{T}_{\alpha\beta}, \quad (7)$$

where the Lorentz matrix is

$$\Lambda^\alpha_\mu = \begin{bmatrix} \frac{1}{\sqrt{1-\omega^2}} & -\frac{\omega}{\sqrt{1-\omega^2}} & 0 & 0 \\ -\frac{\omega}{\sqrt{1-\omega^2}} & \frac{1}{\sqrt{1-\omega^2}} & 0 & 0 \\ 0 & 0 & 1 & 0 \\ 0 & 0 & 0 & 1 \end{bmatrix}. \quad (8)$$

We define

$$\bar{\rho} = \hat{\rho} + 3\hat{\sigma}, \quad \bar{P} = \hat{P} + \hat{\sigma}, \quad \bar{\varepsilon} = \hat{\varepsilon} \frac{1+\omega}{1-\omega}.$$

Note also that from (2-3) the velocity of matter in the radiative coordinates is given by

$$\frac{dr}{du} = \frac{V}{r} \cdot \frac{\omega}{1-\omega^2}, \quad (9)$$

so forth the energy-impulse tensor in the Lorentz system is

$$\begin{aligned}
 \bar{T}_{00} &= \bar{\varepsilon} + \frac{\bar{\rho} + \omega^2 \bar{P}}{1-\omega^2} \\
 \bar{T}_{01} = \bar{T}_{10} &= -\bar{\varepsilon} - \frac{\omega}{1-\omega^2} (\bar{\rho} + \bar{P}) \\
 \bar{T}_{11} &= \frac{\bar{P} + \omega^2 \bar{\rho}}{1-\omega^2} + \bar{\varepsilon} \\
 \bar{T}_{22} = \bar{T}_{33} &= \bar{P}.
 \end{aligned}$$

Using (2) - (5) we obtain the energy-impulse tensor in radiative coordinates as:

$$\begin{aligned}
 T_{00} &= e^{2\beta} \left(\frac{V}{r}\right) \left(\frac{\bar{\rho} + \omega^2 \bar{P}}{1-\omega^2} + \bar{\varepsilon}\right) \\
 T_{01} = T_{10} &= e^{2\beta} \left(\frac{\bar{\rho} - \omega \bar{P}}{1+\omega}\right) \\
 T_{11} &= e^{2\beta} \left(\frac{r}{V}\right) \left(\frac{1-\omega}{1+\omega}\right) (\bar{\rho} + \bar{P}) \\
 T_{22} = \frac{T_{33}}{\sin^2 \theta} &= r^2 \bar{P}.
 \end{aligned}$$

Remember that a bar indicates that the quantity is measured in the Lorentzian system, and the effective variables are written without bar. Now

$$\rho \equiv \frac{\bar{\rho} - \omega \bar{P}}{1+\omega}, \quad P \equiv \frac{\bar{P} - \omega \bar{\rho}}{1+\omega}, \quad \varepsilon \equiv \bar{\varepsilon}. \quad (10)$$

It can be seen at once that $\rho = \bar{\rho}$ and $P = \bar{P}$ in $r = 0$, also, in the static case $\omega = 0$. As before then:

$$\begin{aligned}
 T_{00} &= e^{2\beta} \left(\frac{V}{r}\right) \left[\frac{\omega(\rho + P)}{(1-\omega)^2} + \rho + \varepsilon\right] \\
 T_{01} = T_{10} &= e^{2\beta} \rho \\
 T_{11} &= e^{2\beta} \left(\frac{r}{V}\right) (\rho + P) \\
 T_{22} = \frac{T_{33}}{\sin^2 \theta} &= r^2 \bar{P},
 \end{aligned}$$

thus the field equations are:

$$\begin{aligned}
 -\frac{V}{r^2} \left[\left(2\beta_{,0} - \frac{V_{,0}}{V} \right) - \frac{1}{r} (2V\beta_{,1} - V_{,1} + e^{2\beta}) \right] &= \\
 = 8\pi e^{2\beta} \left(\frac{V}{r}\right) \left[\varepsilon + \rho + \frac{\omega(\rho + P)}{(\omega - 1)^2} \right] & \quad (11)
 \end{aligned}$$

$$2V\beta_{,1} - V_{,1} + e^{2\beta} = 8\pi r^2 e^{2\beta} \rho \quad (12)$$

$$\frac{4\beta_{,1}}{r} = 8\pi \frac{r}{V} e^{2\beta} (\rho + P) \tag{13}$$

$$-2\beta_{,01} + \frac{1}{2r^2} [rV_{,11} - 2\beta_{,1}V + 2r(V_{,1}\beta_{,1} + V\beta_{,11})] = 8\pi e^{2\beta} \bar{P}. \tag{14}$$

Using the conservation equations (Bianchi Identity) $T^\mu_{\nu;\mu} = 0$, we obtain only three no-trivial relations:

$$T^\mu_{1;\mu} = \frac{e^{-2\beta}}{2\pi r} \beta_{,10} - \frac{\partial P}{\partial r} + \frac{1}{2} \left(2\beta_{,1} + \frac{V_{,1}}{V} - \frac{1}{r} \right) (\rho + P) - \frac{2(P - \bar{P})}{r} = 0, \tag{15}$$

$$T^\lambda_{0;\lambda} = \frac{V}{r} \left\{ \left(2\beta_{,1} + \frac{V_{,1}}{V} + \frac{1}{r} \right) \left[\varepsilon + \frac{\omega(\rho + P)}{(1 - \omega)^2} \right] + \frac{\omega}{(1 - \omega)^2} \frac{\partial(\rho + P)}{\partial r} \right\} + \frac{1}{2} \left(2\beta_{,0} - \frac{V_{,0}}{V} \right) (\rho + P) + \frac{\partial \rho}{\partial u} + \frac{V}{r} \left[\frac{\partial \varepsilon}{\partial r} + \frac{1 + \omega}{(1 - \omega)^3} (\rho + P) \frac{\partial \omega}{\partial r} \right] = 0, \tag{16}$$

$$e^{2\beta} T^\lambda_{;\lambda} = \frac{V}{r} \left\{ \left(2\beta_{,1} + \frac{V_{,1}}{V} + \frac{1}{r} \right) \left[\varepsilon + \frac{1 + \omega^2}{2(1 - \omega)^2} (\rho + P) \right] + \frac{\omega(\rho + P)_{,1}}{(1 - \omega)^2} + \frac{\partial P}{\partial r} + \frac{1}{r} [\rho + \bar{P} - (P - \bar{P})] \right\} + \frac{1}{2} \left(2\beta_{,0} - \frac{V_{,0}}{V} \right) (\rho + P) + \frac{\partial P}{\partial u} + \frac{V}{r} \left[\frac{\partial \varepsilon}{\partial r} + \frac{1 + \omega}{(1 - \omega)^3} (\rho + P) \frac{\partial \omega}{\partial r} \right] = 0. \tag{17}$$

It is remarkable that only two Bianchi equations (15-17) are independent, then

$$e^{2\beta} T^\mu_{;\mu} - T^\mu_{0;\mu} = \left(\frac{V}{r} \right) T^\mu_{1;\mu} = 0. \tag{18}$$

If we use the Bondi mass aspect $V \equiv e^{2\beta} (r - 2m)$, after some elementary algebra, the equation system becomes equivalent to:

$$m_{,1} = 4\pi r^2 \rho \tag{19}$$

$$\beta_{,1} = 2\pi r \frac{(\rho + P)}{1 - \frac{2m}{r}} \tag{20}$$

$$m_{,0} = -4\pi r^2 e^{2\beta} \left(1 - \frac{2m}{r} \right) \left[\varepsilon + \frac{\omega(\rho + P)}{(1 - \omega)^2} \right] \tag{21}$$

$$8\pi \bar{P} = -2\beta_{,01} e^{-2\beta} + \left(1 - \frac{2m}{r} \right) \left(2\beta_{,11} + 4\beta_{,1}^2 - \frac{\beta_{,1}}{r} \right) + \frac{1}{r} [3\beta_{,1} (1 - 2m_{,1}) - m_{,11}]. \tag{22}$$

Also, for two independent Bianchi equations (15) and (16), we obtain:

$$-\frac{e^{-2\beta}}{2\pi r} \beta_{,10} + \frac{\partial P}{\partial r} + \left(4\pi r^2 P + \frac{m}{r} \right) \frac{(\rho + P)}{r \left(1 - \frac{2m}{r} \right)} + \frac{2}{r} (P - \bar{P}) = 0, \tag{23}$$

$$\frac{e^{2\beta}}{r} \left[1 + \left(1 - \frac{2m}{r} \right) + 4\pi r^2 (P - \rho) \right] \left[\varepsilon + \frac{\omega(\rho + P)}{(1 - \omega)^2} \right] + \frac{V}{r} \frac{\omega}{(1 - \omega)^2} \frac{\partial}{\partial r} (\rho + P) + \frac{V}{r} \left[\frac{\partial \varepsilon}{\partial r} + \frac{(1 + \omega)(\rho + P)}{(1 - \omega)^3} \frac{\partial \omega}{\partial r} \right] + \frac{\partial \rho}{\partial u} = 0. \tag{24}$$

The expression (23) is the generalization of the Tolman - Oppenheimer - Volkoff (TOV) equation of hydrostatic equilibrium (see, for example [31]). It can be shown that the conservation equation (24) can also be obtained from the field equations (19) and (21), remembering that the second mixed derivatives commute, that is, $m_{,01} = m_{,10}$. Now, combining (21) with (24) we obtain:

$$\frac{2m_{,0} e^{-2\beta}}{4\pi r^3 \left(1 - \frac{2m}{r} \right)} \left[1 - \frac{m}{r} + 2\pi r^2 (P - \rho) \right] = \frac{\omega}{(1 - \omega)^2} \left(1 - \frac{2m}{r} \right) (\rho + P)_{,1} + \frac{\partial \varepsilon}{\partial r} + \frac{(1 + \omega)(\rho + P)}{(1 - \omega)^3} \frac{\partial \omega}{\partial r} + \frac{e^{-2\beta}}{4\pi r^2} m_{,10}.$$

If we assume that radiation profiles ε and the variable ω , vary little, so we can write an expression very similar to the Euler equation

$$2m_{,0} \left[1 - \frac{m}{r} + 2\pi r^2 (P - \rho) \right] = \frac{\omega \cdot e^{2\beta}}{(1 - \omega)^2} \left[4\pi r^2 \left(1 - \frac{2m}{r} \right)^2 r (\rho + P)_{,1} \right] + r \left(1 - \frac{2m}{r} \right) m_{,10}. \tag{25}$$

Equation (25) is omitted in previous works on the evolution of radiating fluid sphere [6, 20, 21, 23, 28]. This omission prevents the closing of the system of equations, and motivates the spurious inclusion of a luminosity Gaussian pulse [21, 23-25, 28]. Equation (25) allows us relate the mass exchange with the time like and radial derivatives of the effective variables, and together with eq. (21), the radiation flux ε

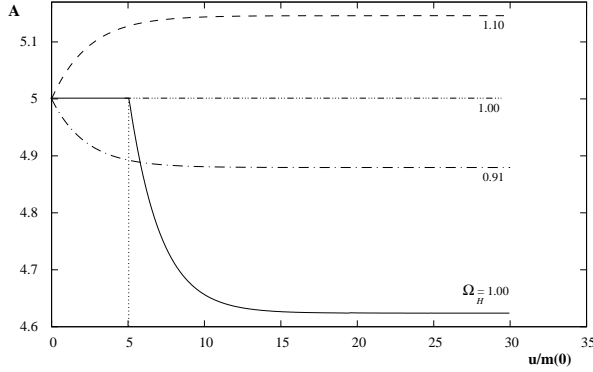


Fig. 1: The radius A as a function of the normalized time-like coordinate $\frac{u}{m(0)}$ for the initial values $A = 5.0$; $M = 1.0$ in the model Schwarzschild-like. Dashed line: $\Omega = 1$ static equilibrium, $\Omega = 1.1$ expansion; $\Omega = 0.91$ collapse. Solid line: solutions according to Herrera et al. [6].

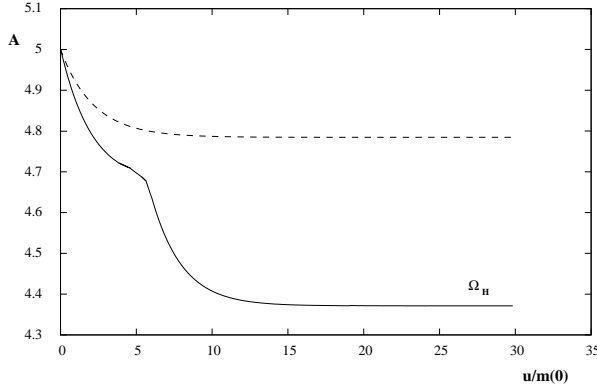


Fig. 2: The radius A as a function of the normalized time like coordinate $\frac{u}{m(0)}$ in the Schwarzschild-like model. Initial values for the surface variables $A = 5$; $M = 1.0$; $\Omega = 0.833$. Dashed line: calculations present. Solid line: solutions according to Herrera et al. [6].

is calculated. With the field equations (19) to (22) we can calculate the expressions of the physical variables ω , \bar{P} , $\bar{\rho}$, if we know the expressions $m(u, r)$ and $\beta(u, r)$ in each layer of the material under study. As a consequence, the state equations $P(u, r)$, $\rho(u, r)$ play an important role in determining the behavior of the physical variables present in the field equations and establishing their posterior evolution.

3 The models and surface equations

From the field equations (19) and (20) we can see

$$m = \int_0^r 4\pi r^2 \rho dr, \quad (26)$$

$$\beta = 2\pi \int_a^r \frac{\rho + P}{1 - \frac{2m}{r}} r \cdot dr. \quad (27)$$

These expressions for m and β are very similar to those obtained in the static case. This suggests a procedure to obtain dynamic solutions, following the same method of Herrera et al. [6], starting from a static solution:

1. Select a static solution of the gravitational field equations for a perfect fluid with spherical symmetry that explicitly shows its radial dependence

$$\rho_{static} = \rho(r) \quad P_{static} = P(r),$$

2. Suppose that the effective variables P and ρ (eq. 10) have the same radial dependence as in the static solution, but taking into account that now the edge condition $\bar{P}_a = 0$ is now expressed as

$$P_a = -\omega_a \rho_a. \quad (28)$$

Note that the subscript Δ_a indicates that the quantity Δ is evaluated at the edge of the distribution.

3. With this radial dependence for the effective variables, and together with (26) and (27), the values of m and β are calculable, except for three unknown functions (surface variables) that we are going to determine:

- (a) Equation (9) evaluated at $r = a$.
- (b) Equation (25) evaluated at $r = a$.
- (c) Equation (15) evaluated at $r = a$, or equation (22) evaluated at $r = a$.

4. Integrating numerically the ordinary differential equations obtained in (3), for a set of initial data, we completely determine the functions m and β .

5. With the field equations (19) to (22) we can calculate the expressions of the physical variables for the model considered.

As outlined in the previous methods (subsection 3), it is necessary to establish the surface variables and the equations that control its evolution.

- As mentioned in (subsection 3a), one of the surface equations is (9) evaluated at $r = a$, which takes the form

$$\dot{a} = \frac{da}{du} = \dot{A} = F(\Omega - 1), \quad (29)$$

where here it is very convenient to standardize the variables in terms of the initial mass $m(0) = m(u = 0, r = a)$ and define as surface variables:

$$A \equiv \frac{a}{m(0)} \quad M \equiv \frac{m_a}{m(0)} \quad \Omega \equiv \frac{1}{1 - \omega_a}, \quad (30)$$

as well as the variable

$$F = \left[e^{2\beta} \left(1 - \frac{2m}{r} \right) \right]_{r=a} = \left(\frac{V}{r} \right)_a, \quad (31)$$

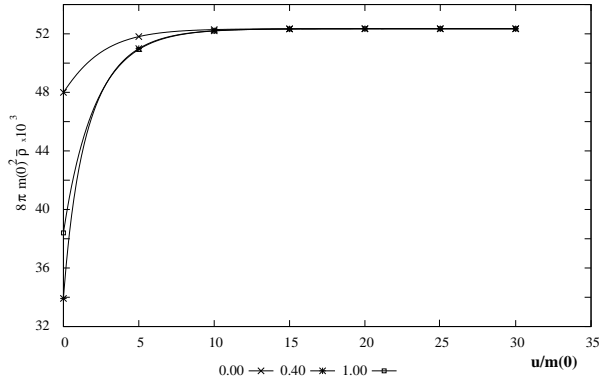


Fig. 3: Density $8\pi m(0)^2 \bar{\rho}$ in function of the temporal variable $\frac{u}{m(0)}$ for the model of Schwarzschild, for $\frac{t}{a} = 0.00, 0.40$ and 1.00 .

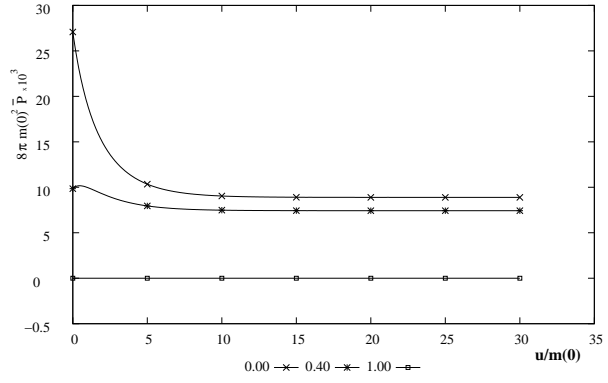


Fig. 4: Normalized pressure values $8\pi m(0)^2 \bar{P}$ in function of the time variable $\frac{u}{m(0)}$ for the model of Schwarzschild, for $\frac{t}{a} = 0.4$ and 1.00

Instead of using as surface variable F (31) – the gravitational potential at the surface –, as used in the references [6, 20, 21, 28]; we will use mass M , that is, the equation for radial evolution is

$$\dot{A} = \left(1 - \frac{2M}{A}\right)(\Omega - 1), \quad (32)$$

This equation is valid for all models.

- The second equation (25) is dependent on the model and it becomes necessary to calculate the first derivatives of the effective density and pressure, as can be seen.

$$\begin{aligned} 2m_{,0}|_a \left\{ 1 - \frac{m}{r} + r\beta_{,1} \left(1 - \frac{2m}{r} \right) - m_{,1} \right\}_a + \\ - r \left(1 - \frac{2m}{r} \right) \frac{\partial}{\partial u} (4\pi r^2 \rho) \Big|_a = \quad (33) \\ = \Omega(\Omega - 1) \left[4\pi r^2 \left(1 - \frac{2m}{r} \right)^2 r \frac{\partial}{\partial r} (\rho + P) \right]_a \end{aligned}$$

- The last equation (23) is the Tolman - Oppenheimer - Volkoff conservation equation evaluated at $r = a$, which we can write

$$\begin{aligned} \beta_{,10}|_a = 2\pi r \left(\frac{\partial P}{\partial r} \right) \Big|_a + \\ + \left[\frac{4\pi r^2 (\rho + P)}{2r^2 \left(1 - \frac{2m}{r} \right)} \right] \left(4\pi r^2 P + \frac{m}{r} \right)_a + \quad (34) \\ + 4\pi (P - P_t)|_a \equiv G. \end{aligned}$$

Both equations (33) and (34) have a similar structure, in terms of the surface variables:

$$\Upsilon_M \dot{A} + \Xi_M \dot{M} + \Lambda_M \dot{\Omega} = \Delta_M \quad (35)$$

$$\Upsilon_\Omega \dot{A} + \Xi_\Omega \dot{M} + \Lambda_\Omega \dot{\Omega} = \Delta_\Omega, \quad (36)$$

where

$$\begin{aligned} \Upsilon_\xi \equiv \Upsilon_\xi(A, M, \Omega), \quad \Xi_\xi \equiv \Xi_\xi(A, M, \Omega), \\ \Lambda_\xi \equiv \Lambda_\xi(A, M, \Omega), \quad \Delta_\xi \equiv \Delta_\xi(A, M, \Omega), \quad \forall \xi \in \{M, \Omega\} \end{aligned}$$

are functions of (A, M, Ω) . These three equations (32), (33) and (34) allow us to establish a system of three ordinary differential equations for the surface variables; which together with the initials data set, determine m and β , as set forth in subsection 4. Below are two examples for the interior distribution Schwarzschild-like and Tolman VI-like in section 4 and 5, respectively.

4 The Schwarzschild-like model

We will get as the first test example Schwarzschild's well-known internal and static constant density solution. For this, we are going to assume that the density depends only on the time-type variable, as explained in [6, 32] we can write the state equation for the Schwarzschild type model as

$$\rho = \frac{3m}{4\pi r^3} \quad (37)$$

$$P = \rho \left\{ \frac{1 - \frac{1}{g} \left[\frac{1 - \frac{2M}{A} \left(\frac{t}{a} \right)^2}{1 - \frac{2M}{A}} \right]^{\frac{1}{2}}}{\frac{1}{g} \left[\frac{1 - \frac{2M}{A} \left(\frac{t}{a} \right)^2}{1 - \frac{2M}{A}} \right]^{\frac{1}{2}} - 3} \right\}, \quad (38)$$

where the value of g is determinated from the boundary condition ($\bar{P}_a = 0$) then the effective pressure satisfies the relationship (28); and consequently $g = \frac{1}{3-2\Omega}$. Evaluating equation (9), for $r = a$, we get (32) and with (23) and (24) for

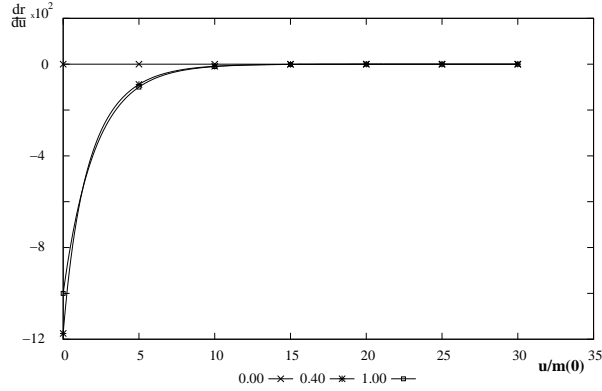


Fig. 5: Temporal velocity evolution in coordinates radiative $\frac{dr}{du}$, for the model of Schwarzschild, for $\frac{z}{a} = 0.00, 0.40$ and 1.00 .

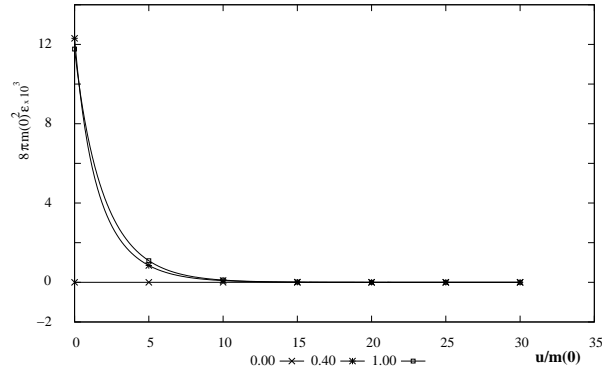


Fig. 6: Radiation profiles $8\pi m(0)^2 \varepsilon$. for the model of Schwarzschild. All layers emit radiation but decrease until reaching a state of equilibrium for $\Omega = 1$.

$r = a$ we obtain then

$$\begin{aligned} \dot{M} &= 3 \left(\frac{M}{A}\right)^2 \left(1 - \frac{2M}{A}\right) \frac{(\Omega - 1)(2\Omega - 3)}{\frac{3M}{A} - \Omega \left(1 + \frac{2M}{A}\right)} \\ \dot{\Omega} &= \frac{2\Omega(1 - \Omega)}{A} \left(1 - \frac{2M}{A}\right) - \frac{1}{A} \left(\frac{M}{A}\right) \left(\frac{3 - 2\Omega}{1 - \frac{2M}{A}}\right) \dot{A} + \\ &\quad - \frac{\Omega}{M} \frac{1}{\left(1 - \frac{2M}{A}\right)} \dot{M}, \end{aligned}$$

and from (20) and (19) we obtain, then after the immediate integration

$$\begin{aligned} m(r) &= m(0) \cdot M \left(\frac{r}{a}\right)^3 \\ \beta &= \frac{1}{2} \log \left[1 + \frac{3}{2\Omega} \left(\sqrt{\frac{1 - \frac{2M}{A}}{1 - \frac{2M}{A} \left(\frac{r}{a}\right)^2}} - 1 \right) \right]. \end{aligned}$$

Figures 1 and 2 show the evolution of the radius A . Notice that $\Omega = 1$ represents a condition of static equilibrium,

$\Omega > 1$ represents expansion, $\Omega < 1$ the collapse. In both cases the system returns to equilibrium very quickly. In order to make some comparison, we took the initial data very close to those chosen in the reference [6]. We did not use the value for $\Omega = 1$, since with this approximation the system does not have static behavior. The figures 3, 4, 5, 6 represent the profiles of physical variables versus the time like coordinates for different pieces of material and for initials data. We obtain monotonous variations in the physical quantities, as a consequence of the non-assumption of the Gaussian pulse. In particular it is shown in figure 6, how all the layers emit monotonously, unlike the figure 7 in Herrera et al. [6]

5 The Tolman VI-like model

Following [2] we can assume as static solution

$$\begin{aligned} 4\pi a^2 \rho &= 3h \left(\frac{a}{r}\right)^2 \\ 4\pi a^2 P &= h \left(\frac{a}{r}\right)^2 \left[\frac{1 - 9 \cdot z \left(\frac{r}{a}\right)}{1 - z \left(\frac{r}{a}\right)} \right], \end{aligned}$$

as before the value of z is determinated from the boundary condition ($\bar{P}_a = 0$) then $P_a = -\omega_a \rho_a$; and consequently $z = \frac{4\Omega - 3}{3(4\Omega - 1)}$; and $h = \frac{m}{3r}$. Evaluating the equations (9), (23) and (24) at $r = a$ we obtain

$$\begin{aligned} \dot{M} &= -\frac{\left(1 - \frac{2M}{A}\right)^2 (16\Omega^2 + 3) \left(\frac{M}{A}\right) \dot{A}}{8 \left[\Omega \left(1 - \frac{2M}{A}\right) + \frac{M}{A} \right]} \\ \dot{\Omega} &= -\frac{1}{A} \left[\frac{M}{A} - \frac{(4\Omega - 3)(4\Omega - 1)}{8} \left(1 - \frac{2M}{A}\right) \right] \\ &\quad + (4\Omega - 1)(4\Omega - 3) \frac{\dot{A}}{8A} + \frac{\Omega}{\left(1 - \frac{2M}{A}\right)} \frac{\dot{M}}{M}, \end{aligned}$$

and the corresponding values of β and m are

$$\begin{aligned} \beta &= \frac{2M}{3A} \frac{1}{\left(1 - \frac{2M}{A}\right)} \left\{ \log \left(\frac{r}{a}\right) + 2 \log \left[\frac{3 - \left(\frac{4\Omega - 3}{4\Omega - 1}\right) \left(\frac{r}{a}\right)}{3 - \left(\frac{4\Omega - 3}{4\Omega - 1}\right)} \right] \right\} \\ m &= m(0) M \left(\frac{r}{a}\right). \end{aligned}$$

Figure 7 shows the temporal variation of the radius of a radiant sphere, for different values of Ω . There is a critical value Ω_0 for $A = 6.66$ and $M = 1$ and slight increase in Ω causes a permanent expansion or the contraction rises to the critical value. In the following figures 8,9,10 we show the variations of pressure density and radiation of some interior layers in case of surface expansion (explosion-like). We noted in the example in the figure 10 that all layers absorbed energy during the initial collapse, an then a radiative pulse is emitted, before returning to the equilibrium configuration.

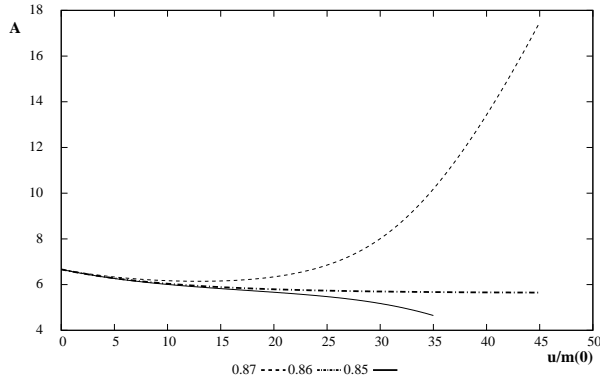


Fig. 7: Radio A of the distribution according to the variable temporary $\frac{u}{m(0)}$ in a TolmannVI-like model. With initials values, $A = 6.66667$; $M = 1$. $\Omega = 0.87$ (rebound) and $\Omega = 0.85$ (contraction) and the critical value $\Omega = 0.860723$

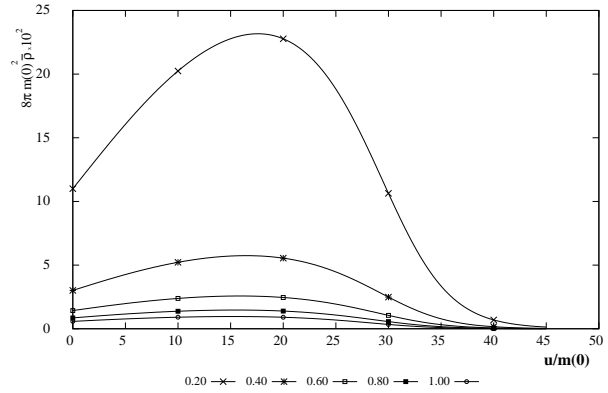


Fig. 9: Density $8\pi m(0)^2 \bar{\rho}$ as function of the time-like variable $\frac{u}{m(0)}$ in a TolmannVI-like model. For the layers in contraction ($\Omega = 0.87$) with $\frac{z}{a} = 0.2, 0.4, 0.6, 0.8$ and 1 .

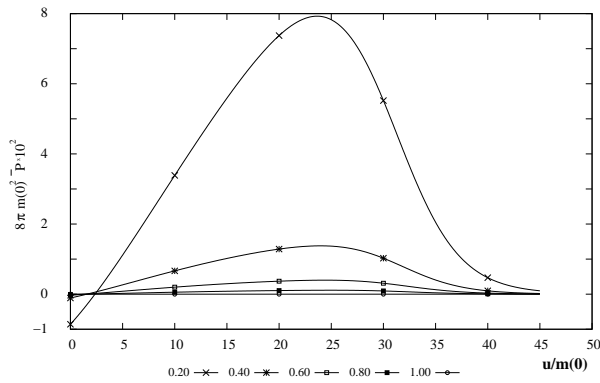


Fig. 8: Values of the normalized pressure $8\pi m(0)^2 \bar{P}$ as function of the time-like variable $\frac{u}{m(0)}$ in a TolmannVI-like model. For the layers in contraction ($\Omega = 0.87$) with $\frac{z}{a} = 0, 0.4, 0.6, 0.8$ and 1 .

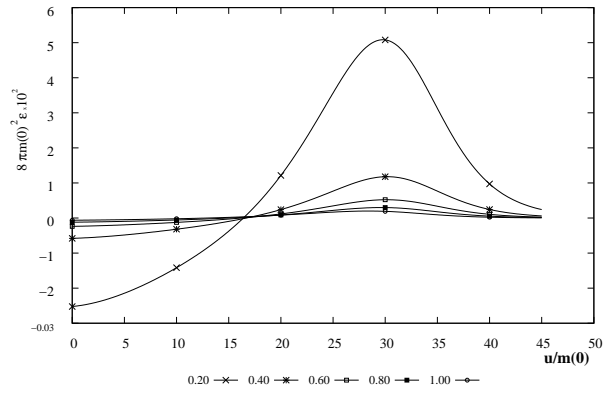


Fig. 10: Radiation profiles emitted $8\pi m(0)^2 \epsilon$ as function of the time-like variable $\frac{u}{m(0)}$ in a TolmannVI-like model. For the layers in contraction ($\Omega = 0.87$) with $\frac{z}{a} = 0.2, 0.4, 0.6, 0.8$ and 1 .

6 Conclusions

We have reviewed the relativistic description of the collapse of self-gravitating radiant spheres, following the usual procedure [6, 19–21, 23, 25, 28, 33] and find that it is an effective method for such a purpose, since the field equations together with the conservation laws (Bianchi’s Identity) form a complete set of integrable equations that do not require an additional hypothesis about the emission of radiated energy. That is, the emission hypothesis of a Gaussian pulse at an arbitrary instant to trigger the collapse; it is not only unnecessary, but also leads to qualitatively and quantitatively different solutions, as we have shown in figures 1-9. We emphasize the importance of using conservation equations properly, as was done in Section 2; We formally reobtain the generalized TOV equation of the hydrostatic equilibrium (equation 23) and a relativistic version of the Euler equation for the self-gravitating sphere (equation 25).

We have seen that the Schwarzschild-like description is an

ideal case that does not represent the phenomenology of the high energy events observed in the stellar collapse of massive stars such as supernovas and quasars. The measurable magnitudes of density, pressure and emission evolve smoothly, returning to the equilibrium condition very rapidly (Figures 3-6). On the other hand, the Tolman VI description involves two possible qualitatively different scenarios, such as the implosion or the explosion of the outer layers of the self-gravitating sphere, depending on the initial values of the mass, radius and velocity observables, as we have shown in figure 7.

We have shown that, in the case of contraction, the density and pressure variables similarly evolve (Figures 8 and 9) as might be expected if a polytrope state equation is used. In addition, Figures 8 and 9, show a dependence of the evolution of such magnitudes according to the radius of the considered layer, with much higher values of density and pressure in the innermost layers, in agreement with the description of the stellar collapse of massive stars.

Finally figure 10 shows that during the collapse of the

self-gravitating radiating spheres a pulse of radiation emission is generated before reaching equilibrium again; which arises *naturally* from the complete solution of the evolution equations, and maybe is important to explain the emission process in very high energy in Supernova bursts and Quasars.

Submitted on January 12, 2018

References

- Oppenheimer J. R. and Snyder H. On Continued Gravitational Contraction. *Physical Review*, 1939, v. 56, 455–459.
- Tolman R. C. Static Solutions of Einstein's Field Equations for Spheres of Fluid. *Physical Review*, 1939, v. 55, 364–373.
- Vaidya P. C. Nonstatic Solutions of Einstein's Field Equations for Spheres of Fluids Radiating Energy. *Physical Review*, 1951, v. 83, 10–17.
- Bondi H. The Contraction of Gravitating Spheres. *Proceedings of the Royal Society of London Series A*, 1964, v. 281, 39–48.
- Bayin, S. Ş Radiating fluid spheres in general relativity. *Phys. Rev. D*, 1979, v. 19, 2838–2846.
- Herrera L., Jiménez J., and Ruggeri G. J. Evolution of radiating fluid spheres in general relativity. *Phys. Rev. D*, 1980, v. 22, 2305–2316.
- Patino A. and Rago H. The Effect of Electric Charge on the Evolution of Radiant Spheres in General Relativity. *Astrophysics and Space Science*, 1996, v. 241, 237–247.
- Sah A. and Chandra P. Class of Charged Fluid Balls in General Relativity. *International Journal of Astronomy and Astrophysics*, 2016, v. 6, 494–511.
- Pant N., Pradhan N. and Bansal R. K. Relativistic model of anisotropic charged fluid sphere in general relativity. *Astrophysics and Space Science*, 2016, v. 361, 41.
- Harko T. and Mak M. K. Exact power series solutions of the structure equations of the general relativistic isotropic fluid stars with linear barotropic and polytropic equations of state. *Astrophysics and Space Science*, 2016, v. 361, 283.
- Maurya S. K. and Maharaj S. D. Anisotropic fluid spheres of embedding class one using Karmarkar condition. *ArXiv e-prints*, 2017.
- Singh K. N., Bhar P., and Pant N. A new solution of embedding class I representing anisotropic fluid sphere in general relativity. *International Journal of Modern Physics D*, 2016, v. 25, 1650099.
- Herrera L. and Falcón N. Heat waves and thermohaline instability in a fluid. *Physics Letters A*, 1995, v. 201, 33–37.
- Herrera L. and Santos N. O. Cylindrical collapse and gravitational waves. *Classical and Quantum Gravity*, 2015, v. 22, 2407–2413.
- Van den Bergh N. and Slobodeanu R. Shear-free perfect fluids with a barotropic equation of state in general relativity: the present status. *Classical and Quantum Gravity*, 2016, v. 33(8), 085008.
- Herrera L., Denmat G. L. and Santos N. O. Dynamical instability and the expansion-free condition. *General Relativity and Gravitation*, 2012, v. 44, 1143–1162.
- Aguirre F., Hernandez H., and Nunez L. A. Radiation hydrodynamics and radiating spheres in general relativity. *Astrophysics and Space Science*, 1994, v. 219, 153–170.
- Chan R., Herrera L., Pacheco J. A. F. and Santos N. O. Diffusion processes in the collapse of a radiating spherical body. *Astrophysical Journal*, 1991, v. 382, 255–260.
- Herrera L. and Barreto W. Relativistic Gravitational Collapse in Co-moving Coordinates: the Post-Quasistatic Approximation. *International Journal of Modern Physics D*, 2011, v. 20, 1265–1288.
- Cosenza M., Herrera L., Esculpi M. and Witten L. Evolution of radiating anisotropic spheres in general relativity. *Phys. Rev. D*, 1982, v. 25, 2527–2535.
- Medina V., Nunez L., Rago H. and Patino A. Evolution of radiating charged spheres in general relativity. *Canadian Journal of Physics*, 1988, v. 66, 981–986.
- Bonnor W. B., de Oliveira A. K. G., and Santos N. O. Radiating spherical collapse. *Phys. Rep.*, 1989, v. 181, 269–326.
- di Prisco A., Falcón N., Herrera L., Esculpi M. and Santos N. O. Pre-relaxation Processes in a Radiating Relativistic Sphere. *General Relativity and Gravitation*, 1997, v. 29, 1391–1405.
- Herrera L., Barreto W., di Prisco A., and Santos N. O. Relativistic gravitational collapse in noncomoving coordinates: The post-quasistatic approximation. *Phys. Rev. D*, 2002, v. 65(10), 104004.
- Barreto W., Rodriguez B., and Martinez H. Radiating Fluid Spheres in the Effective Variables Approximation. *Astrophysics and Space Science*, 2002, v. 282, 581–593.
- Pant N., Mehta R. N., and Tewari B. C. Relativistic model of radiating massive fluid sphere. *Astrophysics and Space Science*, 2010, v. 327, 279–283.
- Tewari B. C. Relativistic collapsing radiating stars. *Astrophysics and Space Science*, 2012, v. 342, 73–77.
- Patiño A. and Rago H. A Sphere Contraction in General Relativity. *Lett. Nuovo Cimento*, 1983, v. 38, 321–328.
- Davies G. Second-Order Black Hole Perturbations: A Computer Algebra Approach, I — The Schwarzschild Spacetime. *ArXiv General Relativity and Quantum Cosmology e-prints*, 1998.
- Neary N., Ishak M., and Lake K. Tolman type VII solution, trapped null orbits, and w-modes. *Phys. Rev. D*, 2001, v. 64(8), 084001.
- Bekenstein J. D. Hydrostatic Equilibrium and Gravitational Collapse of Relativistic Charged Fluid Balls. *Phys. Rev. D*, 1971, v. 4, 2185–2190.
- Aguirre F., Nunez L. A., and Soldovieri T. Variable Eddington Factor and Radiating Slowly Rotating Bodies in General Relativity. *ArXiv General Relativity and Quantum Cosmology e-prints*, 2005.
- Barreto W., Rodríguez B., Rosales L., and Serrano O. Self-similar and charged radiating spheres: an anisotropic approach. *General Relativity and Gravitation*, 2007, v. 39, 537–538.